8C.6

Idealized simulations of the impact of dry Saharan air on Atlantic hurricanes

Scott A. Braun[#], Jason Sippel[#], and David Nolan*

#Laboratory for Atmospheres, NASA/Goddard Space Flight Center, Greenbelt, MD
*University of Miami, Miami, FL

1. Introduction

High relative humidity in the middle troposphere has long been recognized as an important factor in determining where tropical cyclones form (Gray 1975, 1979, 1998; McBride 1981). Its favorable role was viewed more in terms of being a necessary climatological condition rather than being a determining factor in whether or not individual cloud clusters went on to develop into tropical cyclones (McBride 1981; McBride and Zehr 1981). However, DeMaria et al. (2001) showed that the Genesis Parameter (GP), of which mid-level moisture is a part, can provide some useful information on the probability of tropical storm formation and Kaplan and DeMaria (2003) showed that high values of low-level 850-700 hPa relative humidity generally favors rapid intensification of tropical cyclones.

Kimball (2006) examined the impact of dry intrusions in semi-idealized numerical simulations of storm landfall in which idealized moisture perturbations were varied in simulations with initial conditions for Hurricane Danny (1997). Kimball varied both the magnitude of the inner-core moisture anomaly (4 g kg^{-1} variations in peak magnitude, maximum in the boundary layer and decreasing with height) and its size (from 250 to 600 km). As might be expected, an initial vortex with higher moisture content (for fixed size) generally led to more intense storms while more extensive moisture anomalies typically led to increased areal extent of rainbands and a larger area of storm winds (17 m s^{-1}). Kimball claimed that dry air intrusions into systems with smaller moist-envelope extents contributed to weakening of those cases, although the differences in minimum central sea-level pressure were generally less than 5 hPa prior to landfall for the experiments with peak moisture of 19 g kg^{-1} (her A19 simulations). The fact that the moisture perturbations extended into the boundary layer makes the role of mid-level moisture anomalies somewhat ambiguous in these simulations.

Hill and Lackman (2009) performed idealized simulations to examine the impact of environmental moisture on storm size. Using a fixed initial vortex and inner-core thermodynamic conditions (80% relative humidity within 100 km radius), they varied the environmental relative humidity between 20 and 80%. In results that were comparable to Kimball (2006), they found that higher environmental humidities led to increased outer rainband production, larger storms, and broader storm-force wind distributions. In terms of storm intensity, differences between the 20, 40, and 60% relative humidity cases were minimal while the 80% humidity case had a lower minimum central pressure, but nearly identical maximum winds. Their results suggest that the environmental humidity has a critical impact on storm size, but a much smaller impact on storm peak intensity (as

Corresponding Author Address: Dr. Scott A. Braun, NASA/GSFC, Mail Code 613.1, Greenbelt, MD 20771. E-mail: Scott.A.Braun@nasa.gov

measure by conventional parameters such as minimum pressure or maximum wind speed).

The potential negative impact of the Saharan Air Layer (SAL) on the development of tropical cyclones has received considerable attention in recent years (Dunion and Velden 2004; Wu et al. 2006; Jones et al. 2007; Lau and Kim 2007a, 2007b; Wu 2007; Dunion and Marron 2008; Sun et al. 2008, 2009; Reale et al. 2009; Shu and Wu 2009). Dunion and Velden (2004) suggested that the SAL negatively impacts tropical cyclones in the following ways: 1) the enhanced low-level temperature inversion, maintained by radiative warming of dust, suppresses deep convective development; 2) vertical wind shear caused by an increase in the low-level easterlies associated with the AEJ inhibits tropical cyclone intensification; and 3) intrusions of dry SAL air into tropical cyclones foster enhanced cold downdrafts (Emanuel 1989; Powell 1990) and lower the convective available potential energy within tropical cyclones. Braun (2010) found little evidence for this negative influence in a composite of National Centers for Environmental Prediction (NCEP) Global Forecast System (GFS) final analyses for 41 storms. Both storms that strengthened (by 10 m s^{-1} or more) and weakened exhibited comparable African easterly jets, high stability, and substantial dry air in their nearby environments. The most significant differences between strengthening and weakening storms were the magnitude of the initial disturbances and winds in the upper troposphere [as also found by McBride (1981) and McBride and Zehr (1981)].

Because many studies have focused on dry air as a key mechanism for hurricane suppression or weakening (Dunion and Velden 2004; Wu et al. 2006; Jones et al. 2007; Wu 2007; Shu and Wu 2009; Sun et al. 2008, 2009), this study uses a set of idealized simulations to examine the impact of a dry air layer comparable to the SAL. These simulations use an environment with no mean flow. More complex simulations with mean flow, including vertical wind shear, are reserved for a future study. Section 2 describes the model setup and experiments, section 3 describes results using a dry air layer located at varying distances north of the initial vortex, and section 4 describes simulations with dry air surrounding the initial vortex, but with varying moist envelope sizes. Conclusions are given in section 6.

2. Model setup and experiments

This study employs the Advanced Research version of the Weather Research and Forecasting (WRF) modeling system (Version 3.1, Skamarock et al. 2005) to conduct idealized simulations of the interaction of developing tropical cyclones with dry Saharan air. Three grids nesting down to 2-km horizontal grid spacing are employed in order to reasonably represent the convection. The outer grid has a horizontal grid spacing of 18 km and contains 240×240 grid points in the *x* and *y* directions. Two nested meshes are used with the following grid spacings and grid dimensions: 6 km and 120×120, and 2 km and 240×240. All grids use 49 vertical levels with a model top at 20 km. Physics options include the Yonsei University boundary layer scheme (Noh et al. 2003; Hong et al. 2006), the MM5 similarity-theory surface-layer scheme (Zhang and Anthes 1982; Skamarock et al. 2005), the Kain-Fritsch cumulus scheme (Kain and Fritsch 1990, 1993; Skamarock et al. 2005) on the 18-km grid, and the WRF Single Moment 3-class simple-ice cloud microphysics scheme (Hong et al. 2004) on all grids. Radiative processes are not included.

Initial and boundary conditions are derived loosely following Nolan et al. (2007) and Nolan and Rapin (2008). The boundary conditions are doubly periodic. The domain is on an f plane with background Coriolis parameter of f=5.0×10^{-5} s^{-1}. The initial vortex is specified as a modified Rankine vortex with radius of maximum winds of 100 km and maximum winds of 15 m s^{-1} at 4.5 km altitude. The background environment representing non-SAL tropical air is specified by the Dunion and Marron (2008) non-SAL sounding. For the control run (CNTL) that excludes a dry SAL layer, this environment is specified for the entire domain. Several different configurations for the dry SAL layer are utilized. The first, labeled DRY270, places a dry SAL layer at all grid points farther than 270 km (15 grid points on the outer domain) north of the initial storm center. North of this boundary, the relative humidity in the 850-600 hPa layer is set to 25%. Note that composite relative humidity fields for weakening storms in Fig. 13 of Braun (2010) show the dry air typically >400 km from the storm center, so the position of the dry-air boundary is closer to the vortex than is suggested by GFS analyses. Additional simulations, labeled DRY144, DRY90, and DRY0 move the dry-air boundary successively closer to the vortex center until the latter case in which the dry-air boundary is at the center. The final set of simulations involve the placement of the dry SAL layer over the entire domain. In DRYALL0, the dry air extends throughout the vortex. Given that storms typically form within an envelope of moist air, in DRYALL150 and DRYALL75, a moist envelope (the non-SAL sounding) is prescribed from the center of the vortex to a radius of 150 and 75 km, respectively, but is otherwise surrounded by the dry SAL air. A summary of all experiments is given in Table 1.

3. Basic experiments and proximity to the dry layer

The CNTL run with no dry layer starts with an initial minimum central pressure of 1012 hPa and takes about 2 days to reach 1000 hPa (Fig. 1) and begin a more rapid intensification process. By day 7, the central pressure drops to a minimum of 940 hPa and the maximum wind speed reaches ~50 m s^{-1}, remaining approximately steady thereafter. The minimum pressure and maximum wind speed in DRY270 are almost identical to those in the CNTL run, suggesting little impact of the dry air for initial separation distances greater than 270 km. As the separation distance is reduced from 270 km to 144 (DRY144), 90 (DRY90), and 0 km (DRY0), the dry air increasingly slows or delays the intensification of the vortex, although all cases reach approximately the same maximum intensity by the end of the simulations. These results suggest that the dry SAL air can act as a brake on development, but only if it is able to penetrate to very small radius during the early stages of development.

The relative humidity at 3 km altitude from the 18-km grid of the DRY0 simulation is shown for selected times in Fig. 2. The southern half of the vortex is collocated with an area of enhanced humidity (Fig. 2a, resulting from the cool anomaly below the balanced mid-level vortex), and the boundary of the dry SAL air goes through the center of the vortex. The cyclonic winds associated with the vortex extend well into the dry air and, after two days (Fig. 2b), has wrapped this dry air nearly all the way around the vortex. In addition to the southward displacement of dry air, the more moist air initially on the southern side of the vortex gets displaced northward into the SAL air mass. Over time (Figs. 2c, 2d), the dry air gets increasingly wrapped around the vortex and axisymmetrized, lowering the overall relative humidity in the environment of the vortex.

To illustrate the mechanism by which the dry air slows intensification, Figs. 3 and 4 show horizontal distributions of simulated mid-level relative humidity and near-surface radar reflectivity, respectively, for 12 h and 3 days into the simulations from the CNTL and DRY0 cases. At 12 h into the simulation, the CNTL run shows two nearly concentric rings of high relative humidity and reflectivity (Figs. 3a and 4a), an inner ring just inside the initial radius of maximum wind and an outer ring along the edge of a circular cold pool region formed by the initial convection. In contrast, in the DRY0 simulation, dry air has wrapped into the eastern portion of the initial vortex (Fig. 3c), largely suppressing any convection beneath the dry air. As a result, the precipitation (Fig. 4c) is highly asymmetric in the outer convective ring and very limited in the inner ring.

By the end of day 3, the CNTL simulation shows a very symmetric system of tropical storm strength (Figs. 3b and 4b), with a nascent eyewall as well as inner and outer rainband structures. A pool of very high θ_e is found within the nascent eye (Fig. 5a), with low θ_e from cold downdrafts prevalent between ~75-200 km from the center. In the DRY0 simulation (Fig. 4d), although a nascent eyewall is beginning to form, the convection remains highly asymmetric (Fig. 7a), with the major portion of the precipitation in the southwestern quadrant. The only remaining very dry air (<50%) is found at a radius of about 200 km (Fig. 3d). Although the dry air has largely been axisymmetrized, an asymmetry in the relative humidity field exists, with humidities between 70-80% prevalent on the eastern side of the storm compared to higher humidities elsewhere. The cold pool characteristics (Fig. 5c) are not qualitatively different from the CNTL run (Fig. 5a) at this time. Histograms of surface θ_e (Fig. 5b) are very similar except for the warmer tail in the distribution in the CTNL run associated with the higher θ_e at the corners of domain 3 (Fig. 5a). Figure 5d shows histograms of vertical mass flux at 5 km altitude for the CNTL and DRY0 cases. Consistent with the suppression of convection by the intrusion of dry air, considerably less upward mass flux occurs in association with updrafts >1.5 m s^{-1}, which leads to the slower storm development in DRY0. There is also a corresponding decrease in downward mass flux associated with convective and mesoscale downdrafts. Similar evolutions of the DRY164 and DRY90 simulations (not shown) are found with comparable cold pool structures and intensities, but with less intrusion of the dry air, suppression of convection, and asymmetry. These results suggest that dry air inhibits intensification in these simulations primarily by inducing convective asymmetries rather than by causing cold downdrafts that reduce energy available to the storm. The convective asymmetries result in reduced upward mass flux within the storm, reduced radial inflow in the boundary layer, and therefore less spin-up of the tangential circulation (Smith et al. 2009).

As might be expected, the largest impact of dry air is found when the dry layer extends across the entire domain (DRYALL0, Fig. 1). In this case, convection is strongly suppressed for the first several days, with only shallow convection present. Deep convection does not begin until the end of the third day, after which time the vortex begins to intensify. The storm undergoes a period of rapid intensification on the fifth day (Fig. 1), approaching the maximum intensity of the other simulations by the end of the simulation after 8 days.

4. Dependence on initial moist envelope

The DRYALL0 simulation, and even the DRY0 simulation, are generally unrealistic for development of actual tropical disturbances since these disturbances virtually always form within some moist envelope of air associated with easterly waves (Dunkerton et al. 2009). This fact suggests that a more realistic initial condition for an environment with dry air surrounding the vortex would include a moist envelope with at least moderate (>60%) humidity within some radius from the initial storm center. To examine the impact of a moist envelope collocated with the vortex, two experiments have been run in which the dry SAL air (from case DRYALL0) within some radius *R* is replaced by the non-SAL sounding.

Given that the initial radius of maximum wind is 100 km, we test R=150 km and R=75 km. Results from the latter case will be emphasized since both simulations produce similar results.

Figure 3e shows the 3-km level relative humidity at 12 h into the simulation. Initially, moist (>80%) conditions exist only within the small pre-defined region near the storm center, otherwise surrounded by very dry air. Over time, the moist region expands (Fig. 3f) as convection increases winds within the boundary layer, driving larger fluxes of sensible and latent heat. The intensity of the storm as a function of time (Fig. 1) is essentially identical to that in the CNTL case, suggesting that a vortex with even a modest sized moist envelope will not necessarily be adversely affected by dry SAL air even when completely surrounded by the SAL. This result is qualitatively consistent with those of Hill and Lackmann (2009), who found very limited impact on storm intensity of relative humidity outside of their prescribed 100-km radius moist envelope.

The horizontal precipitation structure of the storm at 12-h into the simulation (Fig. 4e) shows suppressed development of the outer convective ring, but several convective cells within an inner convective ring. By 3 days, an eyewall has formed (Fig. 4f), but with a radius that is nearly half that in the CNTL simulation. Cold pools are prevalent within the boundary layer in the storm (Fig. 5e), with a cooler θ_e distribution compared to the CTNL run (Fig. 5b). The downward mass flux is slightly smaller than in the CNTL run (Fig. 5f). Considering the cooler surface θ_e distribution, the smaller downward mass flux likely occurs because of the smaller size of the storm. Likewise, given the very similar storm intensities in the DRYALL75 and CNTL runs (Fig. 1), the reduced upward mass flux is also likely a result of reduced storm size. Despite the significant downdraft activity and cold-pool generation, the storm intensity in the DRYALL75 simulation is essentially identical to the CNTL run.

The dry-air layers in the DRYALL75 and DRYALL150 cases completely surround the initial vortices and are approximately the same distance from the initial vortex centers as in the DRY90 and DRY164 simulations, yet have little impact on storm intensity compared to the latter cases. The results presented above suggest that it is the convective asymmetry induced by the asymmetric ingestion of dry air that acts to slow storm intensification. The ingestion of dry air and any resultant enhancement of cold downdraft activity does not play a primary role in determining storm intensity in the simulations discussed in this paper.

5. Conclusions

This study has focused on a particular aspect of the proposed (Dunion and Velden 2004) negative influences of the Saharan Air Layer on the development of tropical cyclones, specifically the role of low-to-mid level dry air in enhancing cold downdraft activity and suppressing storm development. The WRF model is used to construct idealized simulations of hurricane development with a non-SAL sounding as well as with different configurations of a dry layer (25% relative humidity between 850-600 hPa): 1) a set of simulations with dry air located north of the vortex center by distances ranging from 0 to 270 km and 2) a second set of simulations with dry air completely surrounding the vortex, but with moist envelopes in the vortex core ranging in size from 0 to 150 km in radius.

For the first set of simulations, no impact of the dry air was seen for dry layers located more than 270 km north of the vortex center (~3 times the initial radius of maximum wind). As the dry air boundary was moved closer to the vortex center than 270 km, the vortex tangential flow increasingly wrapped the dry air into the region of convection. The dry air suppressed convective development, leading to increasing asymmetry of the convective vertical mass flux and slower storm development as the dry air boundary was moved closer to the center. Note that all simulations eventually reached the same steady-state intensity. Because convective downdraft activity (as evinced by near-surface θ_e) was similar in all cases, the simulations suggest that the reductions in total vertical mass flux caused by the dry-air induced precipitation asymmetries was the leading cause of the slower storm development.

For the second set of simulations, the presence of dry air throughout the domain, including the vortex center, substantially suppressed storm development, delaying intensification at least two days. However, dry air throughout the vortex is rather unrealistic. Observations suggest that most systems have a pocket or envelope of high humidity within the vortex core. When moist envelopes (consisting of the non-SAL thermodynamic characteristics) were included within the vortex even out to a radius less than the initial radius of maximum wind, the storm intensity evolved in a manner very similar to the control run without dry air, but the storm size was significantly reduced, consistent with the findings of Hill and Lackmann (2009).

The results above suggest that proximity of dry air near or even surrounding a moist vortex should not be interpreted as an indication of potential suppression of tropical storm development. The dry air must approach very close to the inner core of the storm, to a distance comparable to or just outside of the radius of maximum winds, in order to slow the intensification of a developing tropical cyclone (e.g., Shelton and Molinari 2009). Otherwise, the dry air apparently acts only to affect the size of the storm (Kimball 2006; Hill and Lackman 2009).

The simulations in this study were intentionally kept very simple, with no mean flow in the environment of the vortex. It is very possible that the impact of dry air might be significantly enhanced when combined with more complex environments, including the presence of environmental vertical wind shear, which would be expected to increase ventilation of storms (Simpson and Riehl 1958; Cram et al. 2007). A future study will address the added complexity of sheared environments.

Acknowledgements: This work was supported by Dr. Ramesh Kakar at NASA Headquarters with funds from the NASA Hurricane Science Research Program.

References

Braun, S. A., 2010: Re-evaluating the role of the Saharan Air Layer in Atlantic tropical cyclogenesis and evolution. *Mon. Wea. Rev.*, (in press).

Cram, T. A., J. Persing, M. T. Montgomery, and S. A. Braun, 2007: High-resolution simulation of Hurricane Bonnie (1998). Part III: A lagrangian trajectory view on mixing processes between the eye, eyewall, and environment. *J. Atmos. Sci.*, **64**, 1835-1856.

DeMaria, J. A. Knaff, and B. H. Connell, 2001: A tropical cyclone genesis parameter for the Tropical Atlantic. *Wea. Forecasting*, **16**, 219-233.

Dunion, J. P. and C. S. Velden, 2004: The impact of the Saharan air layer on Atlantic tropical cyclone activity, *Bull. Amer. Meteor. Soc.*, 353-365.

Dunion, J. P., and C. S. Marron, 2008: A reexamination of the Jordan mean tropical sounding based on awareness of the Saharan Air Layer: Results from 2002. *J. Climate*, **21**, 5242-5253.

Dunkerton, T. J., M. T. Montgomery, and Z. Wang, 2008: Tropical cyclogenesis in a tropical wave critical layer: Easterly waves. *Atmospheric Chemistry and Physics*, **9**, 5587-5646.

Emanuel, K.A., 1989: The finite-amplitude nature of tropical cyclogenesis. *J. Atmos. Sci.*, **46**, 3431–3456.

Gray, W. M. 1975: Tropical cyclone genesis. Dept. of Atmos. Sci. Paper No. 234, Colo. State University, Ft. Collins, CO, 121 pp.

———, 1979: Hurricanes: Their formation, structure and likely role in the tropical circulation. *Meteorology Over Tropical Oceans*. D. B. Shaw (Ed.), Roy. Meteor. Soc., James Glaisher House, Grenville Place, Bracknell, Berkshire, RG12 1BX, pp.155-218.

———, 1998: The formation of tropical cyclones. *Meteor. Atmos. Phys.*, **67**, 37-69.

Hill, K. A., and G. M. Lackmann, 2009: Influence of environmental humidity on tropical cyclone size. *Mon. Wea. Rev.*, **137**, 3294-3315.

Hong, S.-Y., J. Dudhia, and S.-H. Chen, 2004: A Revised Approach to Ice Microphysical Processes for the Bulk Parameterization of Clouds and Precipitation, Mon. Wea. Rev., 132, 103–120.

Hong, S.-Y., Y. Noh, and J. Dudhia, 2006: A new vertical diffusion package with an explicit treatment of entrainment processes. *Mon. Wea. Rev.*, **134**, 2318-2341.

Jones, T. A., D. J. Cecil, and J. Dunion, 2007: The environmental and inner-core conditions governing the intensity of Hurricane Erin (2007). *Wea. Forecasting*. **22**, 708-725.

Kain, J. S., and J. M. Fritsch, 1990: A one-dimensional entraining/ detraining plume model and its application in convective parameterization, *J. Atmos. Sci.*, **47**, 2784–2802.

Kain, J. S., and J. M. Fritsch, 1993: Convective parameterization for mesoscale models: The Kain-Fritcsh scheme, *The representation of cumulus convection in numerical models*, K. A. Emanuel and D.J. Raymond, Eds., Amer. Meteor. Soc., 246 pp.

Kaplan, J., and M. DeMaria, 2003: Large-scale characteristics of rapidly intensifying tropical cyclones in the North Atlantic basin. *Wea. Forecasting*, **18**, 1093-1108.

Kimball, S. K., 2006: A modeling study of hurricane landfall in a dry environment. *Mon. Wea. Rev.*, **134**, 1901-1918.

Lau, K. M., and J. M. Kim, 2007a: How nature foiled the 2006 hurricane forecasts. *EOS Trans.*, **88**, No. 9, 105-107.

Lau, K. M., and J. M. Kim, 2007b: Cooling of the Atlantic by Saharan dust. *Geophys. Res. Lett.,* **34**, doi:10.1029/2007GL031538.

McBride, J. L., 1981: Observational analysis of tropical cyclone formation. Part I: Basic description of data sets. *J. Atmos. Sci.*, **38**, 1117-1131.

McBride, J. L., and R. Zehr, 1981: Observational analysis of tropical cyclone formation. Part II: Comparison of non-developing versus developing systems. *J. Atmos. Sci.*, **38**, 1132-1151.

Noh , Y., W. G. Cheon, S. Y. Hong, and S Raasch, 2003: Improvement of the K-profile model for the planetary boundary layer based on large eddy simulation data. *Boundary-Layer Meteor.*, **107**, 401-427.

Nolan, D. S., and E. D. Rappin, 2008: Increased sensitivity of tropical cyclogenesis to wind shear in higher SST environments. *Geophys. Res. Lett.,* **35**, doi:10.1029/2008GL034147.

———, ———, and K. A. Emanuel, 2007: Tropical cyclogenesis sensitivity to environmental parameters in radiative-convective equilibrium. *Quart. J. Roy. Meteor. Soc.*, **133**, 2085-2107.

Powell, M.D., 1990: Boundary layer structure and dynamics in outer hurricane rainbands. Part II: Downdraft modification and mixed-layer recovery. *Mon. Wea. Rev.*, **118**, 918–938.

Reale, O., W. K. Lau, K.-M. Kim, and E. Brin, 2009: Atlantic tropical cyclogenetic processes during SOP-3 NAMMA in the GEOS-5 global data assimilation and forecast system. *J. Atmos. Sci.*, **66**, 3563-3578.

Shelton, K. L., and J. Molinari, 2009: Life of a six-hour hurricane. *Mon. Wea. Rev.*, **137**, 51-67.

Shu, S., and L. Wu, 2009: Analysis of the influence of the Saharan air layer on tropical cyclone intensity using AIRS/Aqua data. *Geophys. Res. Lett.,* **36**, doi:10.1029/2009GL037634.

Simpson, R. H., and H. Riehl, 1958: Mid-troposphere ventilation as a constraint on hurricane development and maintenance. *Proc. Tech. Conf. on Hurricanes,* Miami Beach, FL, Amer. Meteor. Soc., D4.1–D4.10.

Skamarock, W. C., J. B. Klemp, J. Dudhia, D. O. Gill, D. M. Barker, W. Wang and J. G. Powers, 2005: A description of the advanced research WRF version 2. *NCAR Technical Note 468+STR*, 88 pp.

Smith, R. K., M. T. Montgomery and S. V. Nguyen, 2009: Tropical-cyclone spin-up revisited. *Quart. J. Roy. Met. Soc.*, **135**, 1321-1335.

Sun, D., K. M. Lau, and M. Kafatos, 2008: Contrasting the 2007 and 2005 hurricane seasons: Evidence of possible impacts of Saharan dry air and dust on tropical cyclone activity in the Atlantic basin. *Geophys. Res. Lett.,* **35**, doi:10.1029/2008GL034529.

Sun, D., W. K. M. Lau, M. Kafatos, Z. Boybeyi, G. Leptoukh, C. Yang, and R. Yang, 2009: Numerical simulations of the impacts of the Saharan Air Layer on Atlantic tropical cyclone development. *J. Climate*, **22**, 6230-6250.

Wu, L., 2007: Impact of Saharan air layer on hurricane peak intensity. *Geophys. Res. Lett.,* **34**, doi:10.1029/2007GL029564.

Wu, L., S. A. Braun, J. J. Qu, and X. Hao, 2006: Simulating the formation of Hurricane Isabel (2003) with AIRS data. *Geophys. Res. Lett.,* **33**, doi:10.1029/2005GL024665.

Zhang, D.-L., and R. A. Anthes, 1982: A high-resolution model of the planetary boundary layer—Sensitivity tests and comparisons with SESAME-79 data. *J. Appl. Meteor.*, **21**, 1594-1609.

Table 1. Simulation names and descriptions.

Simulation Name	Description
CNTL	Control run with uniform non-SAL environment
DRY270	Dry air located northward of 270 km from vortex center
DRY144	Dry air located northward of 144 km from vortex center
DRY90	Dry air located northward of 90 km from vortex center
DRY0	Dry air located northward of vortex center
DRYALL0	Dry air throughout domain, including vortex
DRYALL75	Dry air throughout domain except within 75 km radius
DRYALL150	Dry air throughout domain except within 150 km radius

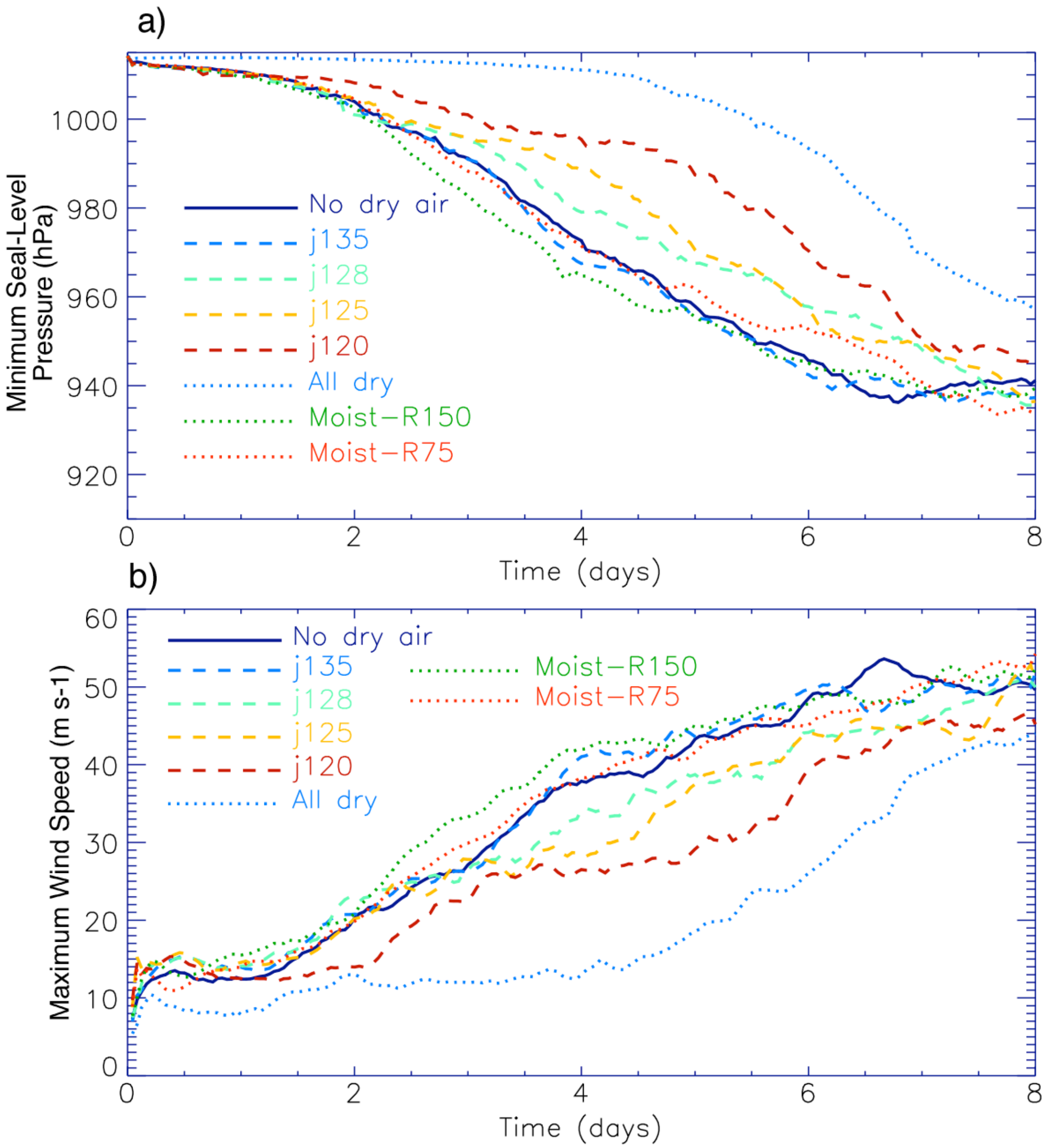

Figure 1. Time series of (a) minimum sea-level pressure and (b) maximum wind speed for all simulations. The solid line is the CNTL run, the dashed lines are the runs with dry air north of a specified latitude, and the dotted lines are for runs with dry air throughout the domain except for a moist envelope within the vortex.

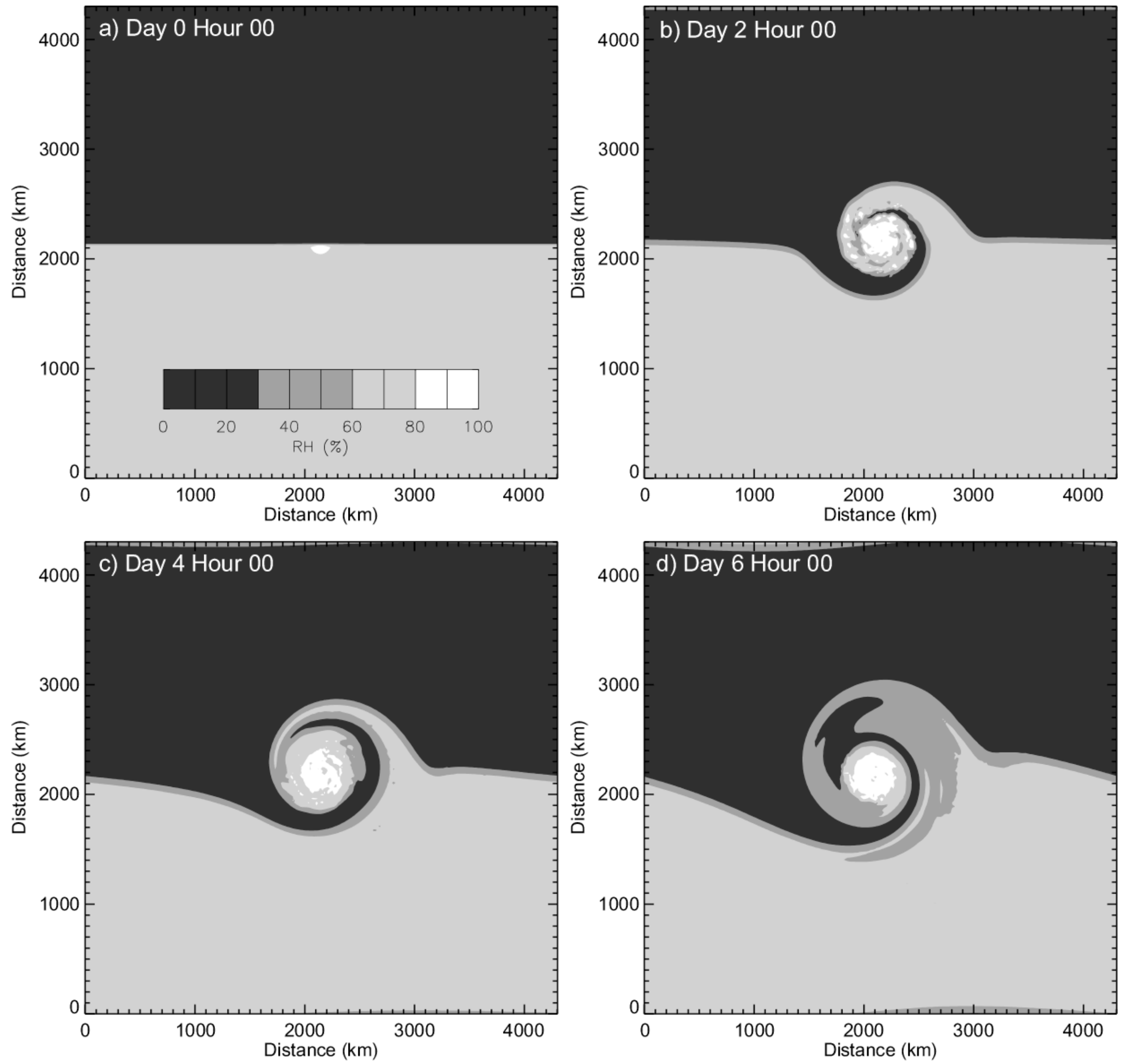

Figure 2. Relative humidity at 3 km altitude from the DRY0 simulation (18-km coarse-grid domain) at (a) the initial time, (b) after 2 days, (c) 4 days, and (d) 6 days. The color scale is shown in panel (a).

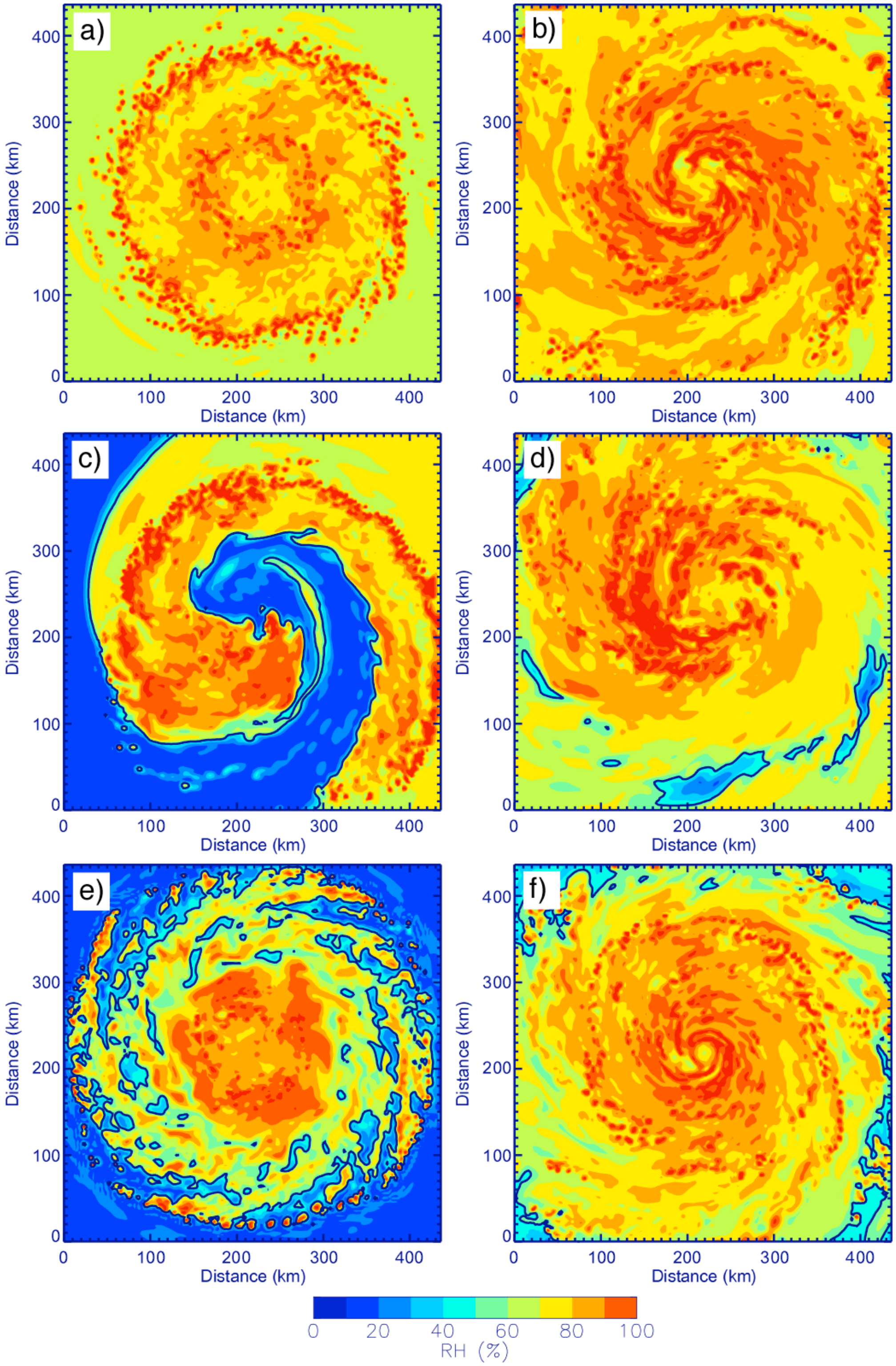

Figure 3. Relative humidity at 3 km altitude from the 2-km resolution domain for (left column) 12 h and (right column) 3 days into the simulation. The top panels are for the CNTL run, the middle panels for the DRY0 simulation, and the bottom panels for the DRYALL75 simulation.

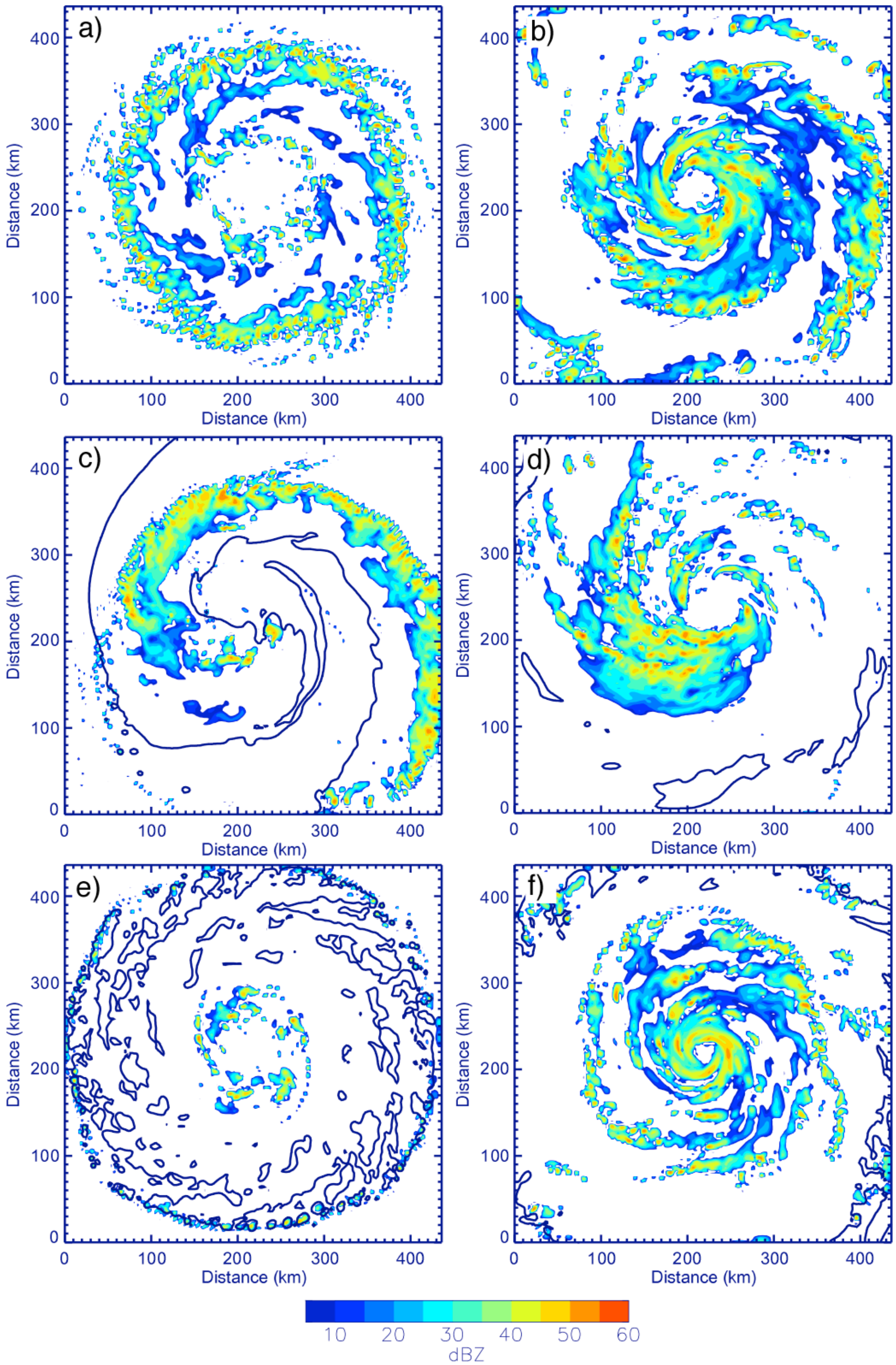

Figure 4. Simulated radar reflectivity at 0.5 km altitude from the 2-km resolution domain for (left column) 12 h and (right column) 3 days into the simulation. The top panels are for the CNTL run, the middle panels for the DRY0 simulation, and the bottom panels for the DRYALL75 simulation. Thick blue contours show the 50% relative humidity contours from Fig. 3.

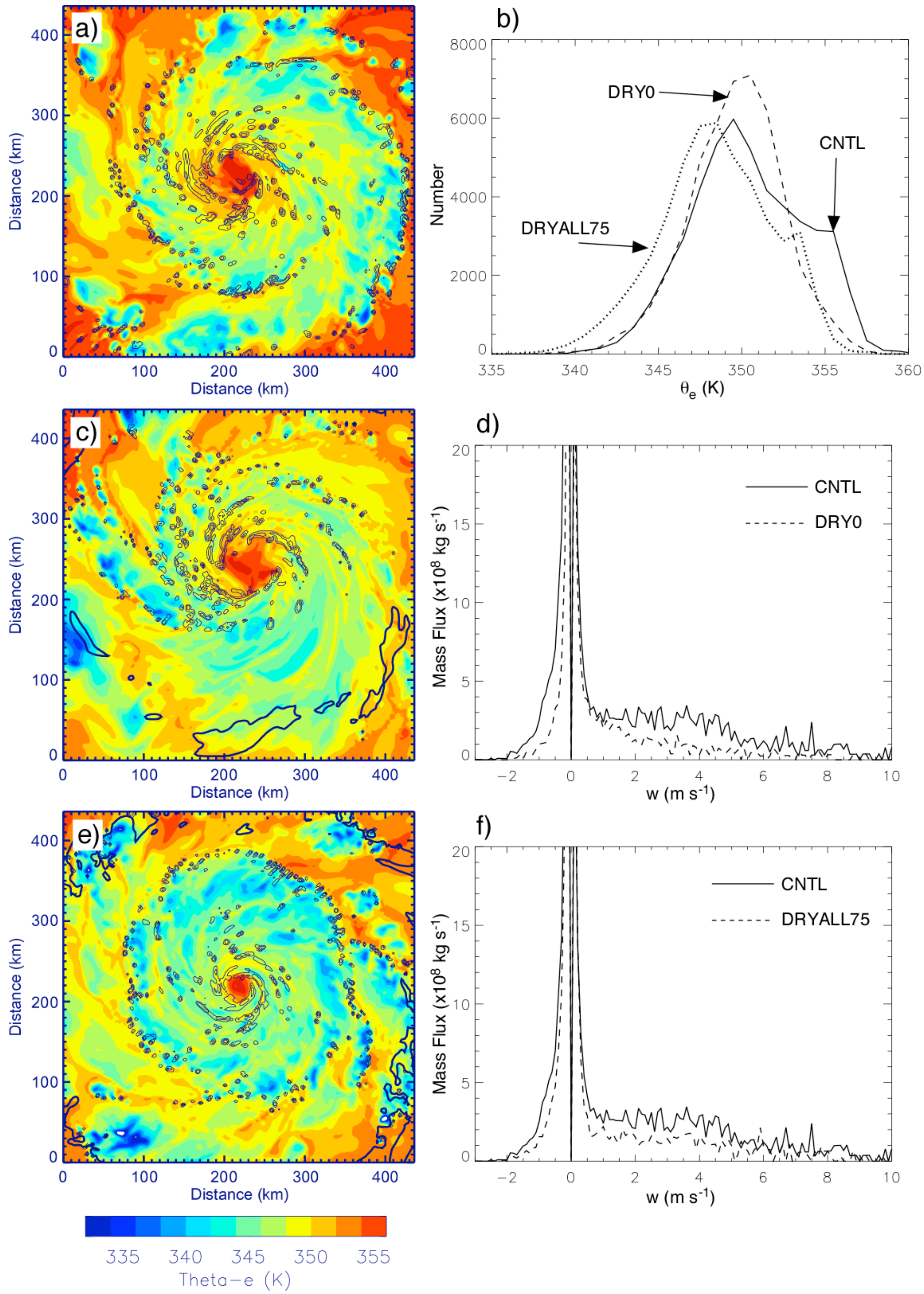

Figure 5. (Left column) Equivalent potential temperature at the lowest model level at 3 days into the simulations. The top panel (a) is for the CNTL run, the middle panel (c) is for the DRY0 simulation, and the bottom panel (e) is for the DRYALL75 simulation. Thick blue contours show the 50% relative humidity contours from Fig. 3. (Right column) In (b), histograms of equivalent

potential temperature from the simulations shown in the left column. (d) Histograms of vertical mass flux at 5 km altitude and 3 days for the CNTL and DRY0 simulations. (f) Same as in (d), but showing the CNTL and DRYALL75 simulations.